Thermally Reprocessable Bio-Based Polymethacrylate Vitrimers and Nanocomposites

Faezeh Hajiali, Saeid Tajbakhsh and Milan Marić*

Department of Chemical Engineering, McGill University, 3610 University St, Montreal, H3A 0C5, Quebec, Canada

Correspondence to: M. Marić (E-mail: milan.maric@mcgill.ca)

Abstract

Vitrimers are covalently cross-linked polymeric materials that can be processed upon heating wherein triggerable polymer networks shuffle chemical bonds through exchange reactions without losing their network integrity. In this work, we apply vitrimers to develop recyclable thermosets derived from materials with relatively high bio-source content. We explore the reaction between ß-ketoesters derived from commercially available (2-acetoacetoxy) ethyl methacrylate (AAEMA) incorporated within isobornyl methacrylate (IBOMA, from pine sap), and a bi-functional amine (Priamine, derived from vegetable oils) to synthesize catalyst-free vitrimers. Controlled radical miniemulsion polymerization was also used to synthesize the water-borne copolymer analogs. Vitrimer nanocomposites were obtained by the incorporation of amine-functionalized polyhedral oligomeric silsesquioxane (POSS-NH_2) at different loadings (0, 5, 10 and 20 wt%). Incorporation of 20 wt% POSS-NH_2 improved tensile modulus (from 96 to 176 MPa), tensile strength (from 2.5 to 5 MPa) and decomposition temperature (225 to 255 °C), and slowed down the relaxation rate and increased apparent activation energy of stress relaxation compared to the neat vitrimer. We further show that the vitrimers studied here and the nanocomposites containing vinylogous urethane cross-linking networks can be un-cross-linked by dissolving in excess mono-functional amine at 65 °C or recycled by grinding and remolding at 125 °C without compromising the mechanical properties.

Keywords: Vitrimers, Nanocomposites, Recyclability, Mechanical and Thermal Properties

Graphical Abstract

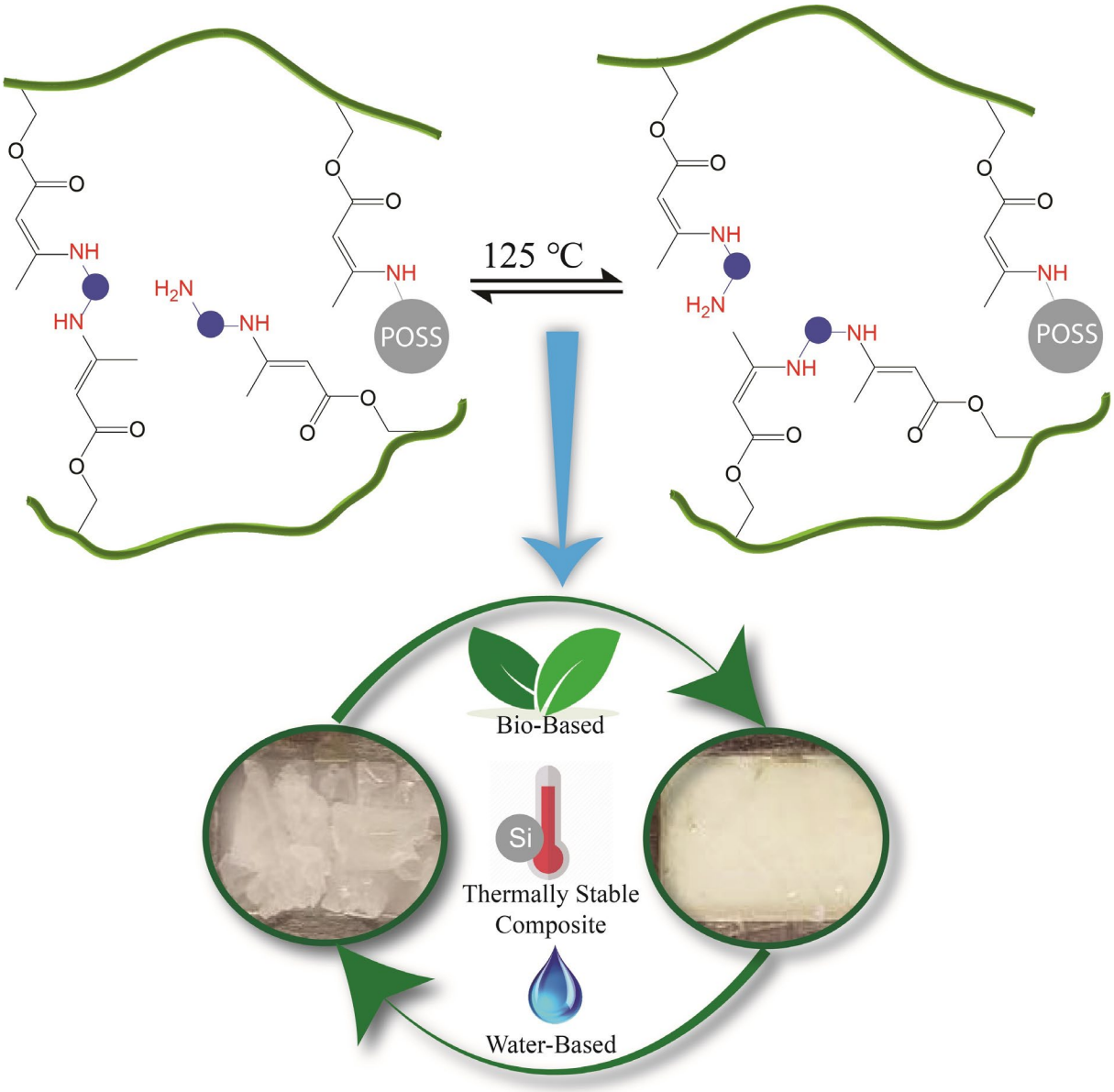

Highlights

- Poly(AAEMA-*stat*-IBOMA) polymers were synthesize by nitroxide-mediated solution and miniemulsion polymerization using Dispolreg 007 without any controlling co-monomer.
- Vitrimers and nanocomposites were fabricated by the Priamine dimer diamine and POSS-NH_2.
- Incorporation of 20 wt% POSS-NH_2 improved thermal and mechanical properties and slowed down the rate of relaxation and increased the activation energy of stress relaxation.
- Vitrimers and nanocomposites were chemically un-cross-linked and mechanically recycled without compromising the mechanical properties.

Introduction

Polymer materials are classically categorized as thermoplastics or thermosets, according to their thermal behavior. Thermoplastics can be easily processed but they are limited by their lower structural stability at high temperatures, strength, abrasion, and solvent resistance. Thermosets, however, are covalently cross-linked materials capable of maintaining their integrity upon heating, and thus possess higher mechanical, thermal and chemical resistance compared to thermoplastics [1]. However, the presence of a permanent network prevents the thermoset from being recycled, melt reprocessed or reshaped [2], giving rise to obvious economic and environmental concerns.

Recently, a new class of thermosets with dynamic cross-links was developed, which can be thermally processed via the introduction of exchangeable chemical bonds, leading to dynamic cross-links. First reported by Leibler and coworkers [3, 4], "vitrimers" are a class of thermosets which behave like permanently cross-linked materials at service temperatures but can flow when heated due to their dynamic cross-linking network. The traditional dynamic network makes use of a *dissociative* cross-link exchange mechanism, in which chemical bonds are first broken and then formed again at another location, resulting in the loss of network integrity. Vitrimers, however, make use of *associative* bond exchanges between polymer chains, in which the original cross-link network is only broken when a new covalent bond to another position has been formed [5]. Thus, the *associative* bond exchange results in a constant cross-linking density without compromising the material properties during reprocessing [6].

Since the pioneering work by Leibler and co-workers in 2011[4], vitrimers have attracted significant research interest [7-13]. The first generations of vitrimers have shown a great potential to bring shape memory [12, 14, 15], malleability[4, 16] and weldability [17] to composites [17], classical epoxy and urethane thermosets [15, 18] and liquid crystalline networks [14, 19]. However, the biggest challenge towards expanding their potential is the fact that the vitrimer concept has to be applied to polymers with

backbones solely comprised of carbon-carbon single bonds as such polymers represent more than 75% of plastics produced every year [7].

So far, a number of catalyst-free vitrimers have been developed which rely on the exchange of vinylogous urethanes [9, 20, 21], vinylogous ureas [20], silyl ethers [22], dioxaborolanes [7], boroxines [23], imines [24] etc. Vitrimers have also been reported which depend on disulfide [25] or olefin [26, 27] exchange groups. Initially reported by Du Prez and coworkers [9], vinylogous urethane vitrimers can be prepared through the condensation reaction of ß-ketoester and primary amines. The vinylogous urethane moieties can undergo dynamic exchanges with available primary amines, which does not need any catalyst and has a negligible exchange rate at room temperature but a rapid one at temperatures above 100 °C [9, 20]. Later, it was demonstrated that the amine exchange of vinylogous urethanes can easily be controlled by using acid and base additives [28]. Recently, Röttger et al.[7] and Lessard et al.[6, 29] showed that poly(methyl methacrylate) (PMMA) could be converted into vitrimers by the incorporation of dioxaborolanes and vinylogous urethanes, respectively. Vinylogous urethane materials could be a promising sustainable cross-linked material, especially if the indefinite recyclability is practical under typical service conditions.

Vitrimer materials that combine a high T_g and improved mechanical properties could prove to be extremely interesting polymer matrices. Particularly, fast exchange kinetics could be a boon in the area of composites [7]. Reinforcement of vitrimers by glass, silica or carbon fibers based on imine exchange [30], transesterification [31], aromatic disulfide [32], and vinylogous urea [20] chemistry have been reported in the literature. Legrand et al. [10] suggested that functionalization of fillers retards the relaxation rate which affects the relaxation-related properties, such as self-healing efficiency of the vitrimers. Zheng et al. [33] demonstrated the synthesis of reprocessable and healable aminated silica/polydimethylsiloxane nanocomposites by vinylogous urethane and Zn(II)-amine coordination bonds into the matrix simultaneously. The nanocomposites revealed the healing efficiency up to 84% after heating at 150 °C for 30 minutes.

Herein, we explore the reaction between ß-ketoesters derived from (2-acetoacetoxy) ethyl methacrylate (AAEMA), a commercially available monomer, incorporated into polymer chain and a bi-functional amine to synthesize catalyst-free vitrimers by using the associative exchange of vinylogous urethanes. We attempted to use commercially available methacrylic monomers and diamines with as much bio-based content as possible. We particularly chose transparent methacrylic polymers as they have several desirable properties such as light weight, high light transmittance, resistance to weathering and good insulating properties [34, 35]. Although AAEMA is petroleum-derived, AAEMA-related monomers can also be partially bio-sourced via the reaction of hydroxyethyl methacrylate (HEMA) and levulinic acid, which is often touted as an important biorefinery feedstock [36]. First, copolymers of AAEMA and isobornyl methacrylate (IBOMA, from pine sap, with 71% bio carbon content) were prepared by nitroxide-mediated polymerization (NMP). NMP was chosen due to its simplicity and the lack of post-polymerization treatment [37, 38]. We employed Dispolreg 007, which was recently shown to be capable of homopolymerizing methacrylates by NMP, without any controlling co-monomer [39, 40]. We explored NMP of poly(AAEMA-*stat*-IBOMA) and studied the polymerization kinetics to verify the nature of AAEMA incorporation. Then, poly(AAEMA-*stat*-IBOMA) copolymer with F_{AAEMA} = 0.53 was converted into networks via a condensation reaction with the dimer diamine (Priamine 1075, 100% renewable carbon content) in one step. Besides the upcycling potential via incorporation of AAEMA and improved thermal stability offered by IBOMA, we added another facet by using nitroxide-mediated miniemulsion polymerization to synthesize water-borne copolymers. Such miniemulsions do not contain volatile organic compounds (VOCs), providing an excellent option for indoor applications [41]. The resulting latex was also treated with the dimer diamine to obtain the vitrimers. We also explored the influence of incorporating amine-functionalized polyhedral oligomeric silsesquioxane (POSS-NH_2) nanoparticles on reprocessability, stress relaxation, gel fraction, mechanical, rheological and thermal properties of the resulting vitrimer nanocomposite. We further show that bio-based vitrimers and the nanocomposites containing vinylogous urethane cross-linking networks can be readily un-cross-linked by dissolving in excess mono-functional amine at 65 °C or recycled by grinding and remolding without compromising the mechanical properties.

The synthesized vitrimers reinforced with POSS could have potential applications in transparent coatings with improved thermal stability. Figure 1 shows the schematic representation of transmission of vinylogous urethanes in this study.

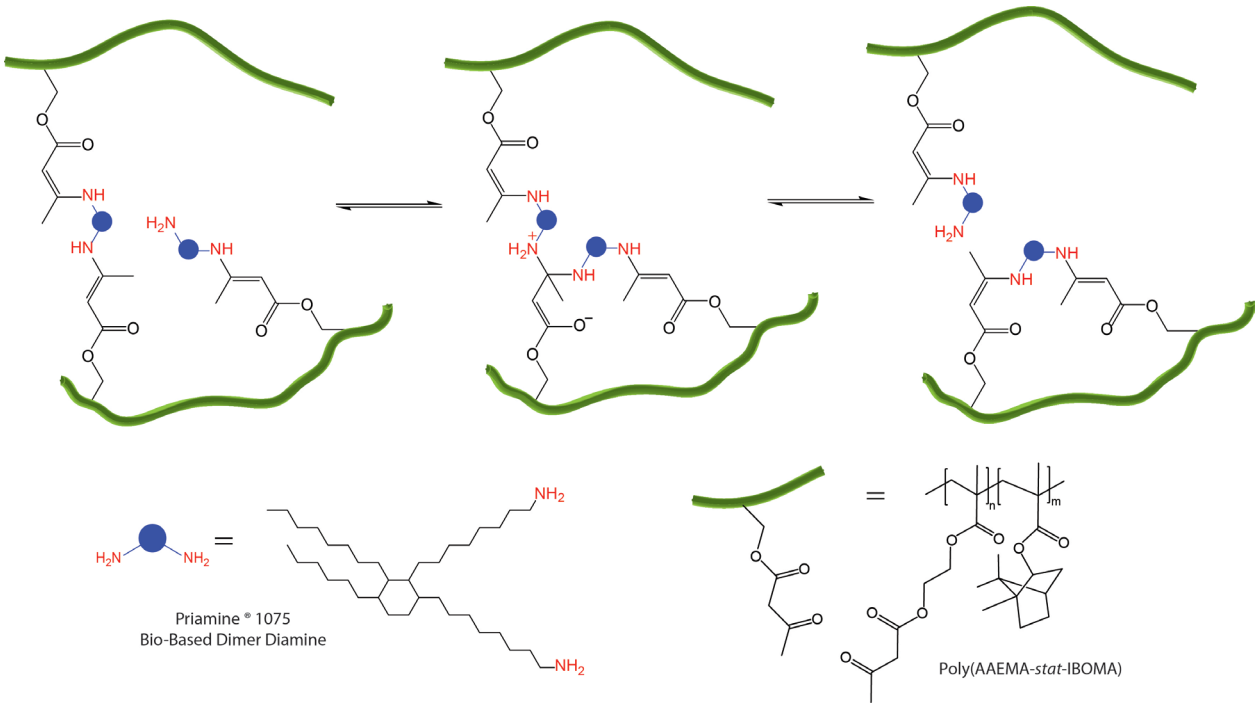

Figure 1. Schematic representation of transamination of vinylogous urethanes between the polymer chains studied in the current work.

Experimental Section

Materials

All chemicals were used as received unless otherwise noted. (2-acetoacetoxy) ethyl methacrylate (AAEMA, Aldrich, 95%) and isobornyl methacrylate (IBOMA, Evonik, >99%, 71% biocontent) were passed through a column of basic alumina to remove inhibitors prior to polymerization. 3-(((2-Cyanopropan-2-yl) oxy) -(cyclohexyl) amino)-2, 2-dimethyl-3-phenylpropanenitrile (Dispolreg 007) was synthesized in the lab according to Ballard et al's procedure [39]. Toluene (ACS), *N,N*-dimethylformamide (DMF, ACS), acetone (ACS), chloroform (HPLC grade, >99.9%) and methanol (>99%) were purchased from Fisher Scientific. The deuterated chloroform ($CDCl_3$, ≥99%) was obtained from Cambridge Isotopes Laboratory for ^1H NMR

tests. DOWFAX™ 8390 (alkyldiphenyloxide disulfonate, 35 wt% active content) was received from Dow Chemical and n-hexadecane (99%) was received from Sigma Aldrich. Priamine™ 1075 with 100% renewable carbon content was purchased from Croda. POSS-NH_2 (~ 3 nm) was obtained from Hybrid Plastics. Butylamine (99%) and acetonitrile (≥99.5%) were purchased from Sigma.

Instrumentation

Gel Permeation Chromatography (GPC). The molecular weight (M_n) and dispersity $Đ$ of polymers were estimated using GPC (Water Breeze) with HPLC grade chloroform as the eluent at 40℃ and a flow rate of 0.3 ml min^{-1} equipped with a guard column, a differential refractive index (RI 2414) detector and three HR Styragel® GPC columns: HR1 with molecular weight measurement range of $10^2 – 5 \times 10^3$ g mol^{-1}, HR 2 with molecular weight measurement range of $5 \times 10^2 – 2 \times 10^4$ g mol^{-1} and HR 4 with molecular weight measurement range of $5 \times 10^3 – 6 \times 10^5$ g mol^{-1}, for chloroform solvent. Samples were diluted in HPLC grade chloroform to a concentration of approximately 5 mg ml^{-1}. Poly(methyl methacrylate) (PMMA) standards were used for calibration (Varian Polymer Standards, molecular weights ranging from 875 to 1677000 g mol^{-1}).

Nuclear Magnetic Resonance (NMR) Spectroscopy. ^{1}H NMR spectra were recorded on a Varian NMR Mercury spectrometer (^{1}H NMR, 300 MHz, 32 scans) with $CDCl_3$ deuterated solvent and DMF as a reference solvent.

FT-IR Spectroscopy. Infrared spectra were collected on a Perkin Elmer Spectrum 2 FT-IR equipped with a single bounce diamond stage attenuated total reflectance (ATR) accessory.

Differential Scanning Calorimetry (DSC). Determination of glass transition temperatures (T_gs) of polymers was performed by a differential scanning calorimetry (DSC, Q2000TM from TA instruments) equipped with an auto-sampler using aluminum hermetically sealed pans. Calibrations for temperature and heat flow were performed using indium and benzoic acid standards, respectively. Ramp experiments were heated at 10 ℃ min^{-1} and cooled at 5 ℃ min^{-1} from -20 to 150 ℃ under nitrogen.

Thermal Gravimetric Analysis (TGA). TGA experiments were performed by a Q500TM from TA instrument equipped with an autosampler using a platinum pan. Each sample was heated to 100 °C isotherm for 30 min prior to each run to remove any possible residual solvent (toluene) or moisture. Isothermal tests were done under nitrogen flow at 10 °C min^{-1} from room temperature to 125 °C, and once at target temperature the experiment was recorded.

Dynamic Mechanical Analysis (DMA) and Rheology. DMA tests were performed using an Anton Paar MCR 302 rheometer. Each rectangular-shaped sample was heated from room temperature to 150 °C at a rate of 5 °C min^{-1}. Sample dimensions were kept consistent for all samples (60 mm length, 10 mm width and 2 mm thickness). All experiments were run at a frequency of 1 Hz. Stress relaxation tests were carried out at 100-130 °C and 1% strain. Strain sweep tests were carried out at a frequency of 1 rad s^{-1} with a 25 mm parallel-plate geometry at 100-130 °C to determine the region of linear response.

Tensile Analysis Testing. The stress-strain analysis of the vitrimers were determined using an MTS Insight material testing system with a 5 kN load cell and a cross-head speed of 10 mm min^{-1}. Dumbbell-shaped specimens (ASTM D638 type V, overall length = 60 mm, overall width = 10 mm) were prepared by solvent casting and hot-press (see Vitrimer Synthesis section for more details).

Polymer Synthesis

In the first set of experiments, statistical copolymerizations of AAEMA and IBOMA were performed at different compositions in order to study polymerization kinetics and the effect of feed composition on the final copolymer composition. Figure 2 shows the general reaction scheme. All experimental formulations can be found in Table 2. As an example, for the experiment AAEMA 50:50 IBOMA, AAEMA (2.60 g, 12.15 mmol), IBOMA (2.70 g, 12.15 mmol), Dispolreg 007 (0.06 g, 0.18 mmol) were added to a 15 ml three-necked round-bottom glass flask containing toluene (6.19 ml, 50 wt% monomer in solvent). The solution was purged with nitrogen prior to being heated at 100 °C for 3 hours. Samples were taken periodically by a syringe until the end of the experiments to be analyzed by ^{1}H NMR and gel permeation

chromatography (GPC). Finally, the reaction was stopped, and the solution was precipitated into methanol and the polymer was dried in vacuum at room temperature for 24 hours. For the specific example cited, the overall ^{1}H NMR conversion was 84% with M_n = 31.3 kg mol^{-1} and $Đ$ = 1.53 (Figure S1 shows ^{1}H NMR spectrum at the end of the reaction for the cited example). Among all the compositions, AAEMA 50:50 IBOMA was chosen for vitrimer synthesis as it is hard enough (due to 50 mol% IBOMA) but can be molded easily due to its relatively low glass transition temperature (T_g = 55 °C).

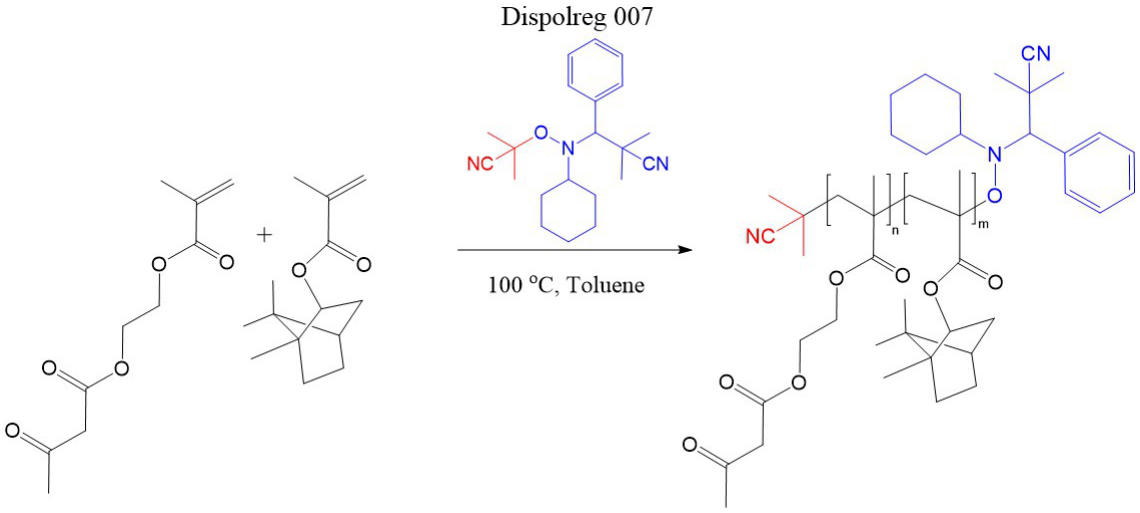

Figure 2. NMP scheme of poly(AAEMA-*stat*-IBOMA) statistical copolymers using Dispolreg 007.

After finding the preferable composition from the solution polymerization studies (i.e. AAEMA 50:50 IBOMA), the copolymerization of AAEMA and IBOMA was conducted in miniemulsion by NMP technique as previously reported by our group [42]. Employing the miniemulsion polymerization avoided the use of organic solvents entirely. First, AAEMA (4.34 g, 20.26 mmol), IBOMA (4.50 g, 20.24 mmol), n-hexadecane hydrophobe (0.07 g) and Dispolreg 007 (0.10 g, 0.29 mmol) were mixed together for 10 minutes. The aqueous phase was prepared separately by dissolving DOWFAX™ 8390 as the surfactant in distilled water by stirring for 10 minutes. The two solutions were then mixed together for 15 minutes and the resulting miniemulsion was sonicated by a Hielscher sonicator UP200S (amplitude 70% and 50% duty cycle) for 10 minutes in a cold water bath and added to a 50 ml three-necked round-bottom glass flask. The reactants were purged with nitrogen for 30 minutes prior to heating at 90 °C for 2 hours. Samples were

taken periodically during the reaction for measurement of particle size (see Figure S5), molecular weight and conversion. All the reported monomer conversions for miniemulsion were measured gravimetrically. Table 1 shows the formulation for the miniemulsion polymerization by NMP.

Table 1. Formulation for the nitroxide-mediated miniemulsion copolymerization of AAEMA and IBOMA

Component	Amount
Monomer (1) – AAEMA	0.542 M
Monomer (2) – IBOMA	0.542 M
Alkoxyamine (Dispolreg 007)	0.008 M
DOWFAX™ 8390	5 wbm%
n-Hexadecane	0.8 wbm%

wbm: weight percent based on the monomers

Vitrimers and Nanocomposites Synthesis

The synthesized AAEMA 50:50 IBOMA solvent-based polymer (F_{AAEMA} = 0.53, 1.0 g, M_n =31.3 kg mol^{-1}) was dissolved in toluene (1.0 g) to reach a solution of 50 wt% polymer in toluene. In a separate vial, Priamine 1075 (0.5 g) was diluted with toluene (2.0 g). The Priamine solution was then added to the polymer and the solution was stirred for 1-2 minutes and then added to the silicone molds (rectangular and dog-bone shaped molds). The same process was repeated for the copolymers made in miniemulsion. After drying the latex, the obtained polymer (1.0 g, M_n = 37.1 kg mol^{-1}) was diluted in toluene (1.0 g) and added to a solution of cross-linker (0.5 g Priamine in 2.0 g toluene). The molar ratio of Priamine to AAEMA was 0.7:1 (mol/mol). This ratio was chosen to provide extra amines for transamination exchange reactions and recyclability of the cross-linked vitrimer. The concept of extra amine was previously discussed by Sumerlin and coworkers [6, 29]. After transferring the solution to the silicone molds, the solvent was evaporated, and the specimens were cured at room temperature for 3 days. As the condensation reaction between ketones and amines generates one equivalent of water, the samples were then post-cured in the oven at 40 °C under vacuum for 6 hours to ensure full curing and dryness. To check the recyclability of the resulting vitrimers, they were ground up and hot pressed at 125 °C and 14 metric tons for up to 6 hours, yielding a transparent material.

The POSS-NH_2-incorporated vitrimer nanocomposites based on different loadings of POSS-NH_2 (0, 5, 10 and 20 wt%) were prepared by solution mixing as indicated in Table 4. For Composite-20, POSS-NH_2 (0.3 g) was first dissolved in toluene (3 g) and added into the solution of polymer/toluene (1.5 g AAEMA 50:50 IBOMA, 1.5 g toluene). Next, the cross-linker solution (0.75 g Priamine in 2.0 g toluene) was added and mixed with the polymer and the final solution was transferred to the silicone molds to make rectangular and dog bone-shaped specimens. The same curing and recycling procedure were used as described earlier. The structure of amine-functionalized POSS-NH_2 and its reaction with ketone groups are shown in Figure 3.

Results and Discussion

Poly(AAEMA-*stat*-IBOMA) Synthesis and Characterization

We began our investigation by preparing statistical copolymers of AAEMA and IBOMA to study the polymerization kinetics. Nitroxide mediated polymerization (NMP) was adopted to synthesize copolymers with desired target molecular weights and well-defined controlled structures. Previously, Sumerlin and coworkers [6] used the RAFT technique to obtain well-defined polymers to be further treated with amines for vitrimer synthesis. However, the RAFT process was challenging since the polymer chains terminated by the thiocarbonylthio chain transfer agent were prone to rapid aminolysis upon treatment with primary amines. Therefore, they employed a post-polymerization treatment to replace the reactive thiocarbonylthio chain ends with inert cyanopropyl groups.

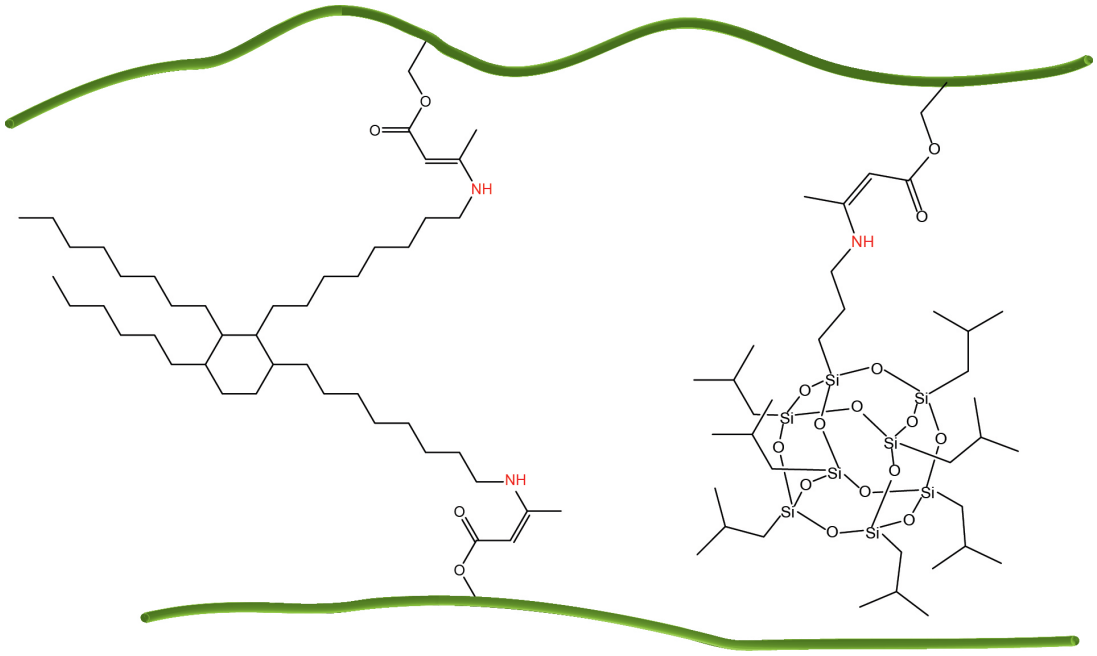

Figure 3. Schematic representation of reaction of aminopropylIsobutyl POSS and Priamine™ dimer diamine with ketone groups.

In the first set of experiments, various statistical copolymers of AAEMA and IBOMA were synthesized using Dispolreg 007 initiator at 100 °C targeting $M_{n,theo}$= 30 kg mol^{-1} with an initial AAEMA molar fraction, f_{AAEMA}, ranging from 0.1 to 0.9. The kinetic plots and the molecular characterization of the resulting copolymers are presented in Figure 4. Characterization of copolymers by both GPC and ^{1}H NMR spectroscopy confirmed that the copolymerization was well-controlled in terms of linear M_n versus conversion and low $Đ$. In AAEMA-rich compositions, the $Đ$ showed a tendency to broaden with conversion. According to Asua and coworkers [39], such an increase in $Đ$ is due to low molecular weight chains (Figure S2) which are consistently present to varying extents during the polymer synthesis and affect $Đ$ as chain length increases. Such low molecular weight tails could be arising from continuous initiation of chains due to the slow dissociation of Dispolreg 007 [43] combined with slow propagation from cyanoalkyl center [44] and/or termination reactions causing dead chains [39]. Although not studied here explicitly, chain end fidelity does not seem compromised in polymerizations with Dispolreg 007, as successful block copolymer synthesis has been reported elsewhere, despite the relatively broad molecular weight

distributions [45-47]. The copolymerization rate increases slightly with increasing AAEMA ratio. According to the literature, the propagation rate constant, k_p, of AAEMA is 3723 L mol^{-1} s^{-1} and k_p of IBOMA is 3589 L mol^{-1} s^{-1} at 100 °C [48, 49]. In addition to kinetic studies, thermal studies were performed and revealed the glass transition temperature (T_g) of samples ranged from 15 to 90 °C by increasing IBOMA from 10 mol% to 90 mol% (Table 2 and Figure S3). The corresponding reactivity ratios were determined via the Meyer and Lowry method, based on the work done by Skeist, fitting the evolution of f_{AAEMA} with the overall molar conversion. This method takes into account the composition drift of the monomer feed during the polymerization [49-51].

$$1 - \frac{M}{M_0} = 1 - \left[\frac{f_1}{f_{1,0}}\right]^{\alpha}\left[\frac{f_2}{f_{2,0}}\right]^{\beta}\left[\frac{f_{1,0}-\delta}{f_1-\delta}\right]^{\gamma}$$

$$\alpha = \frac{r_2}{1-r_2}, \beta = \frac{r_1}{1-r_1}, \gamma = \frac{1-r_1 r_2}{(1-r_1)(1-r_2)}, \delta = \frac{1-r_2}{2-r_1-r_2} \qquad (1)$$

Using equation 1, the reactivity ratios obtained were r_{AAEMA} = 1.43 ± 0.05 and r_{IBOMA} = 0.79 ± 0.03, by minimizing the error between the theoretical and experimental data. This suggests that AAEMA is slightly more reactive than IBOMA toward both propagating species which could be resulting in a weakly gradient copolymer (Figure 4d). For comparison, Zoller et al. [49] reported a complete kinetic analysis of AAEMA and AAEMA/MMA copolymerization, demonstrating a strong increase of copolymerization rate with increasing AAEMA content. The reactivity ratios of AAEMA/MMA copolymerization at 75 °C in ethyl 3-ethoxypropionate (EEP) were found to be close to unity (r_{AAEMA} = 0.98 and r_{MMA} =0.89) by the Meyer–Lowry method, suggesting an essentially random copolymer structure. Reactivity ratios for oxidative copolymerization of AAEMA with St and MMA calculated by the Kelen-Tüdös method indicated r_{AAEMA} = 0.095, r_{st} = 8.65 and r_{AAEMA} = 0.57, r_{MMA} = 0.66, respectively [52].

Table 2. AAEMA/IBOMA statistical copolymerization formulation with molecular and thermal characterization for various compositions

ID	$[Dispolreg]_0$ (M)	$[AAEMA]_0$ (M)	$[IBOMA]_0$ (M)	$[Toluene]_0$ (M)	$f_{AAEMA,0}$[a]	F_{AAEMA}[b]	$Đ$[c]	M_n[c] ($kg\ mol^{-1}$)	X[d] (%)	T_g (°C)
AAEMA 10:90 IBOMA	0.015	0.208	1.871	5.054	0.10	0.11	1.39	23.5	81	90

AAEMA 20:80 IBOMA	0.015	0.420	1.679	5.083	0.20	0.22	1.43	24.2	83	84
AAEMA 30:70 IBOMA	0.016	0.635	1.483	5.112	0.30	0.32	1.55	28.1	80	77
AAEMA 40:60 IBOMA	0.016	0.855	1.283	5.142	0.40	0.44	1.54	26.7	84	60
AAEMA 50:50 IBOMA	0.016	1.080	1.080	5.173	0.50	0.53	1.53	31.3	84	55
AAEMA 60:40 IBOMA	0.016	1.308	0.872	5.204	0.60	0.62	1.63	33.5	86	40
AAEMA 70:30 IBOMA	0.016	1.541	0.660	5.235	0.70	0.71	1.67	32.5	87	34
AAEMA 80:20 IBOMA	0.016	1.779	0.445	5.267	0.80	0.82	1.70	33.2	87	25
AAEMA 90:10 IBOMA	0.016	2.021	0.225	5.300	0.90	0.90	1.77	35.2	90	15

[a] Initial molar fraction of AAEMA in the feed, [b] molar fraction of AAEMA in final polymer, [c] Đ and number-average molecular weight (M_n) of the polymer determined by GPC relative to PMMA standards at 40 ℃. [d] Final monomer conversion determined by ^{1}HNMR.

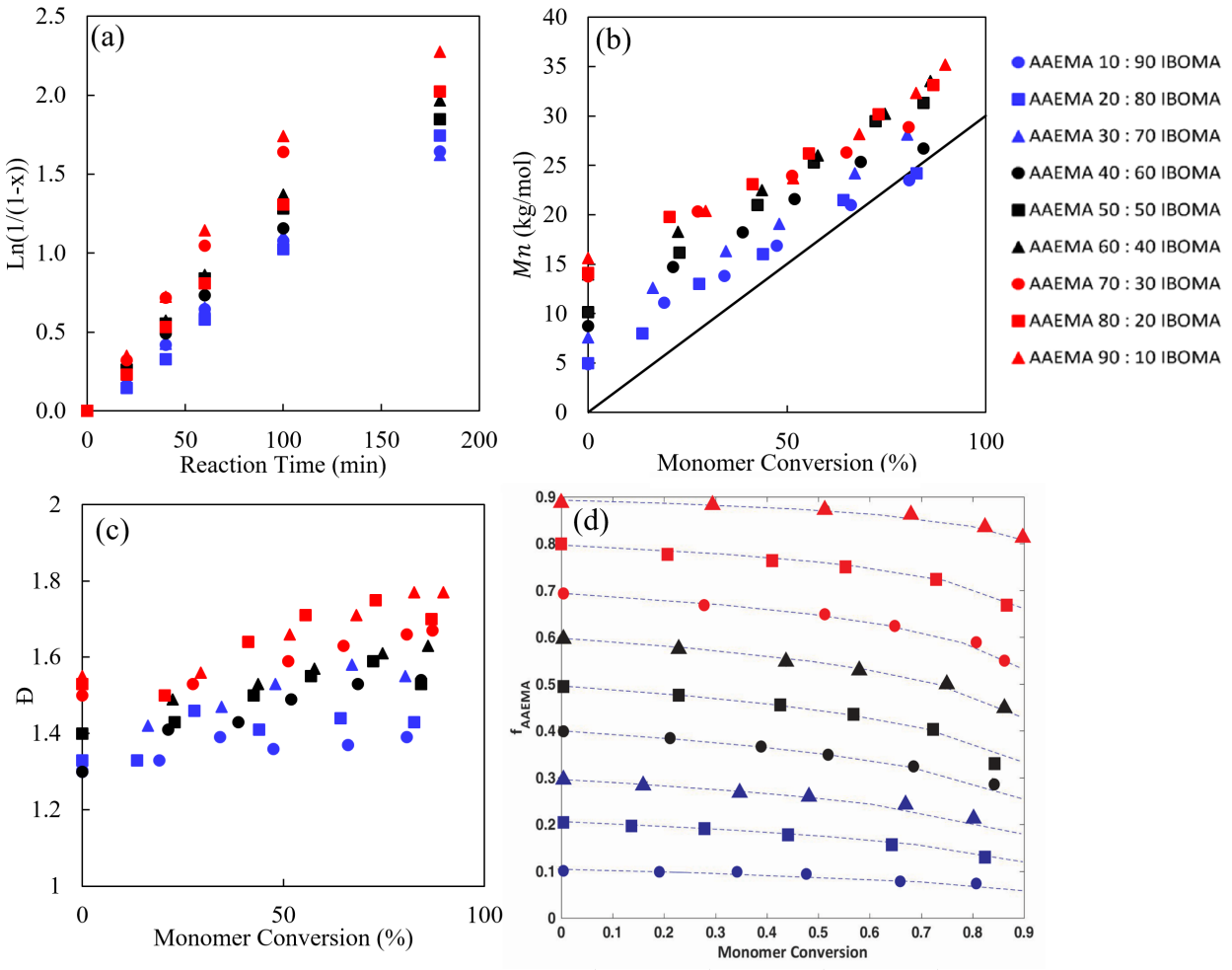

Figure 4. (a) Semi-logarithmic kinetic plots of ln[(1-x^{-1})] (x= monomer conversion) versus reaction time and (b) number average molecular weight, M_n, and (c) dispersity $Đ$ versus conversion for NMP of AAEMA/IBOMA. (d) AAEMA molar feed (f_{AAEMA}) versus overall molar conversion of monomers.

Theoretical lines were calculated with r_{AAEMA} = 1.43 and r_{IBOMA} = 0.79. All experimental ID and characterization of experiments are listed in Table 2.

After completing the kinetic studies, the composition containing 50 mol% AAEMA (AAEMA 50:50 IBOMA) was selected for further experiments as it contains enough IBOMA to achieve desirable mechanical and thermal properties while also retaining sufficient cross-linkable units to promote facile exchange. In addition to solution polymerization, we conducted polymerization in dispersed aqueous media (Figure 5). Accordingly, we were able to reach a total conversion in miniemulsion (92%) comparable to the solution polymerization (84%). According to Figure 5, the polymerization obeyed first-order kinetics and the growth of molecular weight remained uniform with monomer conversion and $Đ$s were between 1.14-1.65. Table 3 compares the molecular characterization of the solvent-based and water-based copolymers.

Table 3. Comparison of molecular characterization of solvent-based (S) and water-based (W) poly(AAEMA-*stat*-IBOMA)

ID	$f_{AAEMA,0}$[a]	F_{AAEMA}[b]	$Đ$[c]	M_n (kg mol^{-1})[c]	X (%)[d]
Poly(AAEMA-*stat*-IBOMA)-S	0.5	0.53	1.53	31.3	84
Poly(AAEMA-*stat*-IBOMA)-W	0.5	0.44	1.65	37.1	92

[a] Initial molar fraction of AAEMA in the feed, [b] molar fraction of AAEMA in final polymer, [c] Đ and number-average molecular weight (M_n) of the polymer determined by GPC relative to PMMA standards at 40 °C. [d] Final monomer conversion determined by ^{1}HNMR.

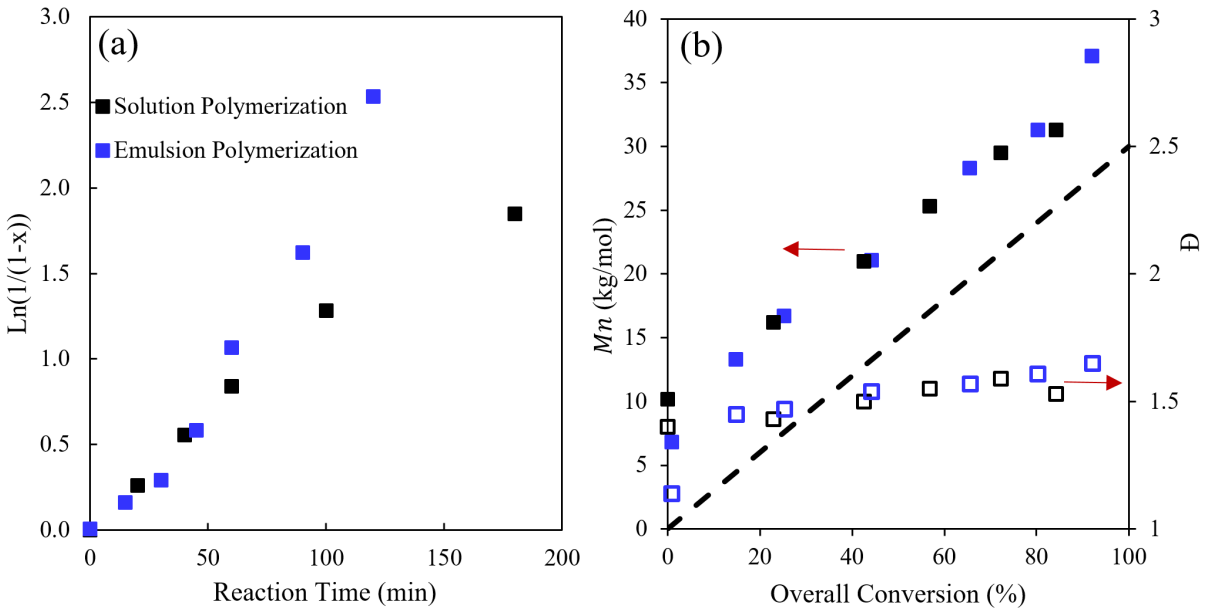

Figure 5. Comparison of solution polymerization and miniemulsion polymerization of AAEMA 50:50 IBOMA using NMP. (a) Semi-logarithmic kinetic plots of $\ln[(1-x)^{-1}]$ (x= monomer conversion) versus polymerization time for solution (■) and miniemulsion (■) polymerization, (b) number average molecular weight, M_n, and dispersity $Đ$ versus conversion for solution (■, □) and miniemulsion (■, □) polymerization.

Vitrimers and Nanocomposites Synthesis and Characterization

After the synthesis of AAEMA 50:50 IBOMA copolymers, they were converted to vitrimers using a bi-functional amine (Priamine™ 1075) by a solution casting method. First, a solution of poly(AAEMA-*stat*-IBOMA) in toluene was treated with Priamine at room temperature. Then, the resultant solution was transferred to silicone molds and evaporated at room temperature and post-cured in an oven to yield homogeneous vitrimer specimens with rectangular and dog-bone shapes (hereinafter referred as Vitrimer-S (made by solution polymerization) and Vitrimer-W (made by miniemulsion polymer in dispersed aqueous media).

As outlined in the Introduction, one of the major applications where the unique properties of vitrimers can be an asset is for composites. Nanoparticles have often been used to improve the mechanical and thermal properties of polymers [53, 54]. Recently, incorporation of fillers to vitrimers and recyclability of the resulting composites have attracted a lot of attention as a thermoset substitute for the development of reshapable, weldable and recyclable composites [10, 55-59]. Thus, POSS-NH_2 nanoparticles were incorporated here through the reaction of the ketone from AAEMA units and the amine group from POSS-NH_2 in order to improve the thermal stability and mechanical properties of the resulting material. We experienced challenges with incorporating POSS via suitable methacrylate functionalization and free radical copolymerization (eg. low ceiling temperature and steric hindrance) [60]. Attaching POSS in a post-polymerization step (Figure 3) was much more facile and allowed us to take advantage of POSS's hybrid structure (useful for compatibilization) and its smaller size compared to other fillers (<10 nm, good for transparency) [61, 62].

A series of vitrimer nanocomposites based on different loadings of POSS-NH_2 (0, 5, 10 and 20 wt%) was prepared as described in the experimental section (molar ratios of POSS-NH_2 to AAEMA are given in Table 4). Formation of vinylogous urethane groups was then confirmed by FTIR spectroscopy for the vitrimers (see *Supplementary Information* for the full spectra). According to Figure 6a, the bands at 1655 cm^{-1} and 1600 cm^{-1} correspond to N-H bending and C=C stretching, respectively. The peak around 1720 cm^{-1} arises from C=O bonds [63]. According to Figure 6a, S13 to S15, the bands at 1655 cm^{-1} and 1600 cm^{-1} correspond to N-H bending and C=C stretching, are stronger for composite compared to vitrimer-S. In addition, the bands at 1100 cm^{-1} and narrow band at 780 cm^{-1} are associated with the Si−O−Si and Si−C stretching vibrations of the POSS, respectively, which indicates that POSS has existed in the composite [64, 65].

Figure 6c and d show tensile stress-strain curve and TGA curves of Vitrimer-S and nanocomposites with different POSS-NH_2 loadings. The data summarizing the mechanical and thermal properties are listed in Table 4. Composite-20 showed superior mechanical properties with tensile modulus of 176 ± 6 MPa and tensile strength of 4.96 ± 0.21 MPA, T_{dec} of 255°C and 2.4 wt% ash content. The low ash content for some POSS-incorporated polymers has been previously observed in the literature [66]. Vitrimer-S showed the lowest modulus, strength, T_{dec} and ash content and highest elongation at break. Vitrimer-S and Composite-20 were then chosen for recycling experiments. Although not the key focus here, it is worth mentioning that the bio-based carbon content of the synthesized Vitrimer-S and nanocomposites were crudely estimated by taking into account the bio-based carbon content of constituting components in the final formulation [67].

Table 4. Comparison of tensile and thermal properties of Vitrimer-S and nanocomposites

ID	POSS-NH_2 (wt%)	POSS-NH_2: AAEMA (mol/mol)	Priamine : AAEMA (mol/mol)	Young's Modulus (MPa)	Stress at break (MPa)	Strain at break (%)	T_{dec}[a] (°C)	Ash Content[a] (wt%)	Bio-based Carbon Content[b] (%)
Vitrimer-S	0	0:1	0.7:1	96 ± 3	2.54 ± 0.11	5.12 ± 0.08	225	0	66
Composite-5	5	0.02:1	0.7:1	106 ±7	2.81 ± 0.18	4.94 ± 0.13	240	0.9	65
Composite-10	10	0.05:1	0.7:1	130 ± 5	3.19 ± 0.25	4.77 ± 0.17	240	1.4	65

Composite-20	20	0.09:1	0.7:1	176 ± 6	4.96 ± 0.21	4.70 ± 0.21	255	2.4	64

[a] T_{dec} and Ash Content measured by TGA under nitrogen flow at a ramp rate of 10 °C min^{-1}. [b] Bio-based carbon content was estimated by considering that AAEMA can be partially renewable as mentioned in the introduction.

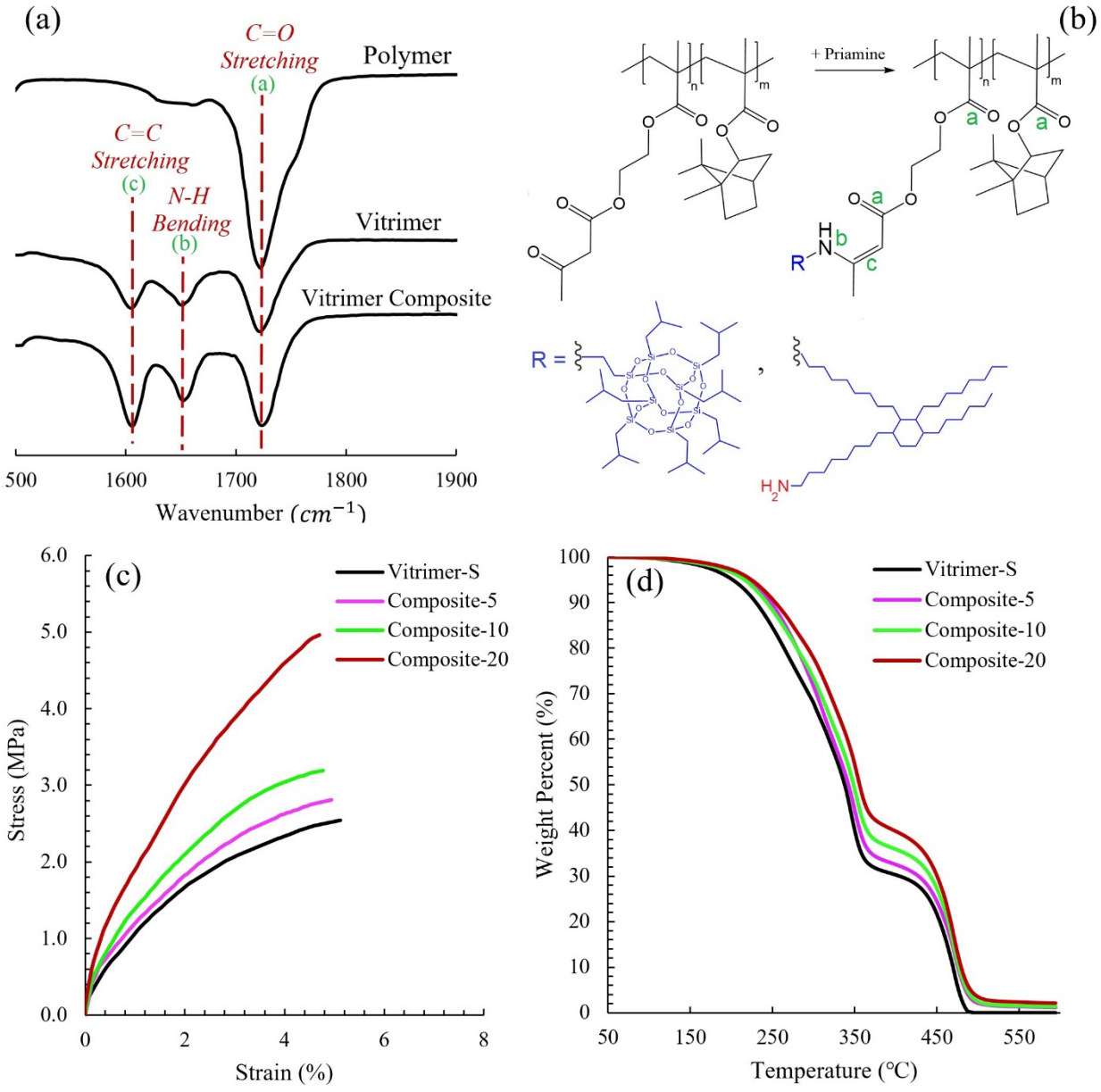

Figure 6. FTIR spectra of poly(AAEMA-*stat*-IBOMA) polymer, Vitrimer-S and Composite, indicating the appearance of vinylogous urethanes after cross-linking with Priamine™ 1075 dimer diamine.

Stress Relaxation of the Vitrimer-S and Composite

As previously reported in the literature, fillers can affect the activation energies of stress relaxation at elevated temperatures and, as a result, affect the vitrimer recovery [10, 55, 58, 68]. We thus investigated the stress relaxation behavior of the vitrimer and the influence of POSS nanoparticles on it. Figure 7a compares the rates of stress relaxation at 110 ℃ for both samples. As expected, the network composite exhibits slower stress relaxation compared to the neat network. For instance, the time required to relax to 37% (1/e) of the initial stress at 110 ℃ increases from 9 s in Vitrimer-S to 21 s in Composite. Overall, the samples showed rapid relaxation behavior which is similar to some studies literature [69]. For instance, aminated silica/PDMS vinylogous urethane vitrimer nanocomposites revealed fast relaxation time ~20 s at relatively low temperatures of 110 ℃. Furthermore, the stress of all PDMS vitrimer composites levelled off after 1200 s indicating the presence of vinylogous urethane crosslinks acting as permanent crosslinks, which is similar to the present study [33]. In another study, the relaxation time was as low as 12 s at 170 ℃ for a bio-based vitrimer epoxy [12]. According to Du Prez and coworkers [70], adjusting the stoichiometry and catalysts can control relaxation times over the range of four orders of magnitude, down to ultrafast relaxation times below one second.

It should be noted that the mono-functionalized POSS cannot participate in the dynamic exchanges during network rearrangement as it has only one functional group attaching to the silsesquioxane cage. According to Torkelson and coworkers [55], when nanofillers have surface functional groups that can participate in dynamic exchanges with the network matrix, recycling leads to losses in mechanical properties along with faster rates and lower apparent activation energy of stress relaxation compared to the neat network at elevated temperatures. However, using non-reactive nanofillers lacking significant levels of functional groups exhibit slower rates with higher apparent activation energy of stress relaxation and higher recovery after recycling compared to functionalized nanoparticles. Indeed, the incorporation of nanofillers in the polymer matrix reduces the network's mobility as fillers serve as non-flowable solids anchored to the polymer chains. Nanoparticles may also block some functional groups on the polymer chains from

contacting with each other and thus reducing the probability of dynamic exchanges [55, 71]. Yet, in this study, even with high filler loadings (20 wt %) the nanocomposites are able to relax at elevated temperatures (see Figure S9) as previously observed in similar studies [10, 68]. As shown in Figure 7b, the system relaxation can be fit to an Arrhenius type relationship using a characteristic relaxation time (τ), which is the time required for stress to relax to 1/e of its initial value at the given temperature. The activation energy was thus extracted from the slope of ln(τ) versus 1000/T (see *Supplementary Information* for calculation details) [72]. The activation energy for Vitrimer-S and Composite was calculated to be 56 kJ mol^{-1} and 70 kJ mol^{-1}, respectively. This is in good agreement with the values previously reported for vinylogous urethane-based vitrimers (55-81 kJ mol^{-1}) [9, 28].

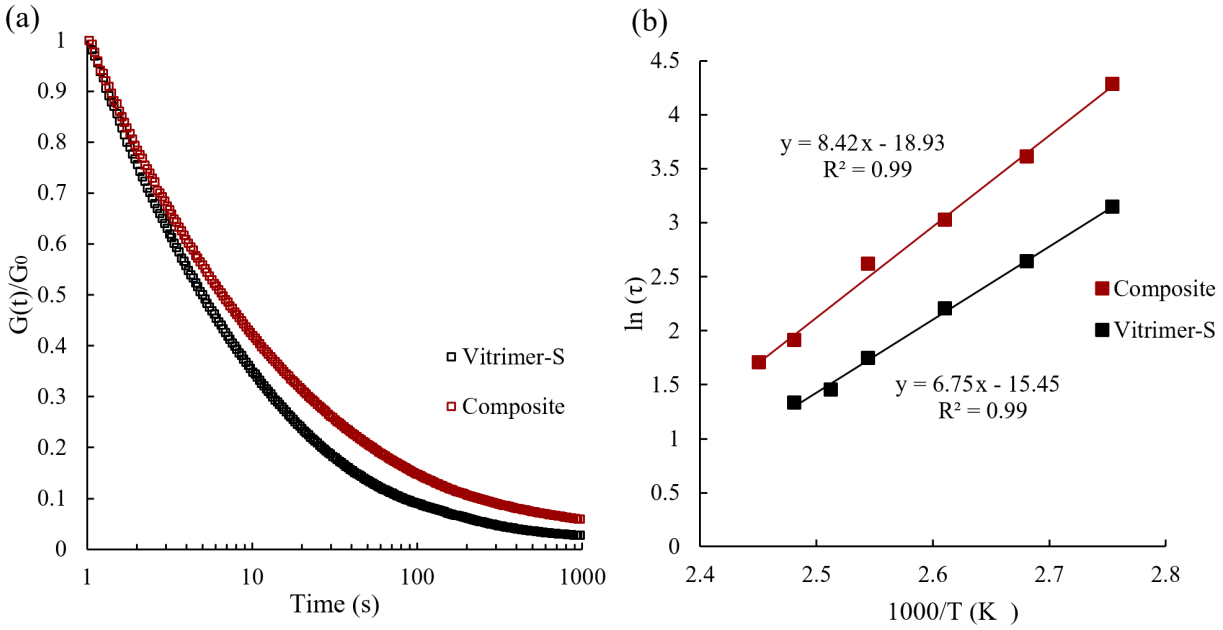

Figure 7. (a) Stress relaxation curves of neat Vitrimer-S and Composite at 110 °C and a strain of 1%. (b) Arrhenius plots obtained from stress relaxation values at G/G_0 =1/e at various temperatures for Vitrimer-S and Composite obtained from Figure S9.

Vitrimers and Nanocomposite Recycling

After preparation of the vitrimers, they were reprocessed at 125 °C and under a pressure of 14 metric tons by hot-press molding up to 6 hours. It is well-known that most of the thermoplastics are usually processed

at temperatures above 200 ℃ [73, 74]. According to Du Prez and coworker [74], processing the NMP-based polymers at such high temperatures (above 200 ℃), results in side reactions due to the reactive chain-end radical promoted by flowing and diffusion of the polymer chains. This might eventually degrade the properties of the final product. In addition, previous studies showed that decomposition of nitroxide groups occurs at temperatures above 200 ℃ [74-77]. However, in the present work, we intentionally chose lower recycling temperature (125 ℃) to avoid/minimize the side reactions caused by the active chain ends. We lowered the recycling temperature by targeting lower glass transition temperatures compared to the similar studies on the methacrylate-based vitrimers [6, 29].Thermogravimetric analysis (TGA) was conducted in order to determine the thermal stability of cured samples under the recycling conditions. Figure S6 in *Supplementary Information* shows little isothermal degradation (< 4%) over 6 hours at 125 ℃ under nitrogen flow which could be due to the water release of the condensation reaction [9]. Comparable studies on the uncross-linked polymer did not show any degradation under the same recycling conditions (Figure S11 and S12). Thus, the neat vitrimers and nanocomposite were reprocessed mechanically by grinding and hot-pressing at 125 ℃ and 14 metric tons to yield recycled bars for further testing as shown in Figure 8. Samples were recycled three times and the retention of network integrity was investigated through DMA, FTIR and tensile tests (Figures 9,10).

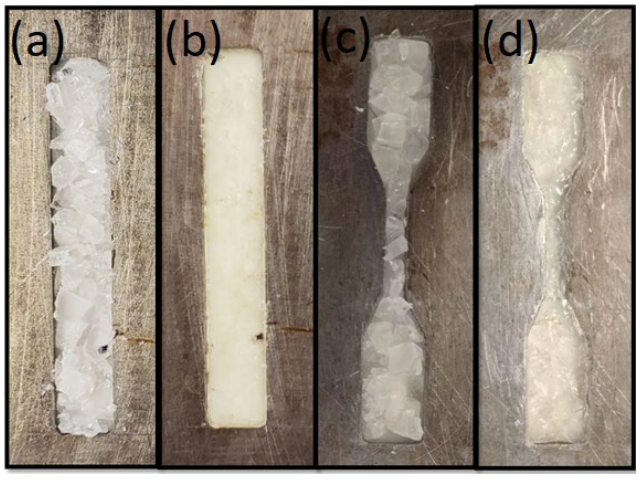

Figure 8. Recycling process of poly(AAEMA-*stat*-IBOMA) vitrimer. Rectangular and dog-bone shape bars: (a, c) after being ground and (b, d) after being hot-pressed at 125 ℃ and 14 metric tons for 6 hours.

DMA experiments (Figure 9) show the storage modulus and T_g of the specimens (59-61 °C for Vitrimer-S, 58-60 °C for Vitrimer-W, and 79-82 °C for Composite) throughout the recycling steps. The storage modulus of the Composite at room temperature (438 MPa) was higher than the neat vitrimers (225 MPa for Vitrimer-S and 350 MPa for Vitrimer-W). DMA confirmed the presence of a network with a rubbery plateau of 0.29 MPa for Vitrimer-S, 0.55 MPa for Composite and 0.43 MPa for Vitrimer-W. The retention of network integrity upon recycling was further proven through the lack of appreciable changes in storage modulus and T_g after reprocessing. Notably, the first reprocessed samples exhibited a rubbery plateau modulus enhanced relative to the original samples which could be due to the formation of additional crosslinks within the system according to the literature [55] and has been observed in similar vinylogous urethane vitrimer studies [6, 29]. The average recovery of mechanical properties for Vitrimer-S (93%) and Vitrimer-W (91%) were slightly higher than the Composite (88%), which is in good agreement with similar studies [6, 78, 79] (between 80-90% for the neat and reinforced vinylogous urethane networks). In addition, FTIR showed no noticeable degradation after successive recycling cycles and the peaks corresponding to vinylogous urethanes are retained after recycling (please see *Supplementary Information* for complete FTIR spectrum).

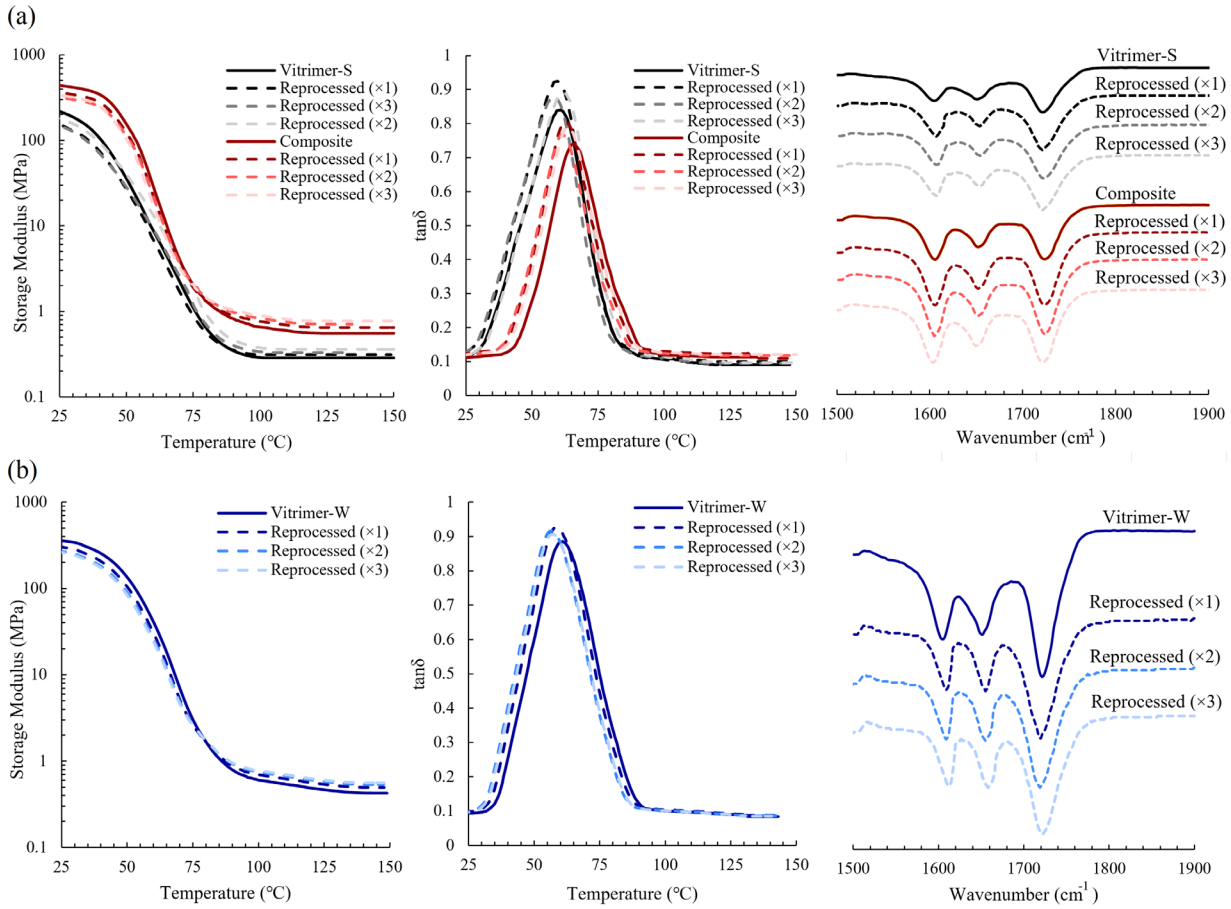

Figure 9. Reprocessing and characterization of vitrimer networks: Storage modulus, tan δ (from DMA) and FTIR spectra of (a) Vitrimer-S and composite, and (b) Vitrimer-W, showing the retention of vinylogous urethane cross-links in the recycled samples.

Figure 10 and Table 5 compare the tensile properties of specimens after 0 to 3 recycling cycles. Tensile tests were achieved at room temperature before each recycling step. Among all the original and recycled samples, Composite exhibited the highest and Vitrimer-S had the lowest tensile properties. The less elastic nature in the Composite could be due to the bulky structure of POSS-NH_2 groups causing a decrease in the entanglement of polymer chains [63]. The tensile properties between Vitrimer-S and Vitrimer-W is marginally different which could be due to the different IBOMA content and slightly higher molecular weight in Vitrimer-W and consequently small differences of tensile properties [80]. Upon the first reprocessing step, a decrease of 10-13% was observed in stress at break and tensile modulus in all samples.

However, after additional recycling steps, the stress at break and Young's modulus reaches a plateau. This drop in mechanical properties could be due to an insufficient healing step and the lack of free amines as previously observed in the literature [69, 81].

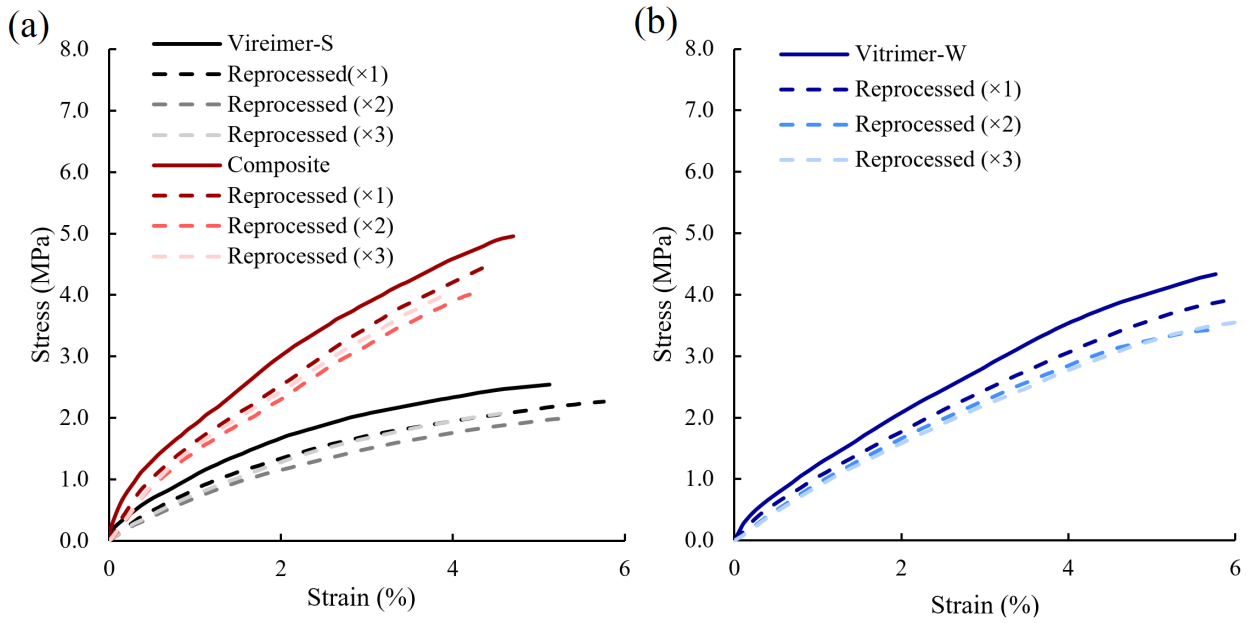

Figure 10. Stress-strain curves of Vitrimer-S, composite and Vitrimer-W for different reprocessing cycles.

Table 5. Tensile properties of vitrimers after 0 to 3 reprocessing.

ID	Young's Modulus (MPa)				Stress at break (MPa)				Strain at break (%)			
	×0	×1	×2	×3	×0	×1	×2	×3	×0	×1	×2	×3
Vitrimer-S	96 ± 3	83 ± 2	70 ± 5	75 ± 2	2.54 ± 0.11	2.27 ± 0.16	1.99 ± 0.13	2.08 ± 0.17	5.12 ±0.08	5.75 ± 0.14	5.35 ± 0.17	4.59 ± 0.12
Vitrimer-W	110 ± 5	99 ± 7	94 ± 3	87 ± 5	4.33 ± 0.17	4.04 ± 0.21	3.43 ± 0. 14	3.61 ± 0.20	5.77 ± 0.12	6.53 ± 0.22	5.77 ± 0.15	6.30 ± 0.17
Composite	176 ± 6	159 ± 8	148 ± 5	155 ± 6	4.96 ± 0.21	4.50 ± 0.24	4.01 ± 0.18	3.99 ± 0.14	4.70 ± 0.21	4.42 ± 0.15	4.20 ± 0.21	3.87 ± 0.16

We also investigated the chemical un-cross-linking by dissolving the cross-linked polymer in presence of an excess mono-functional amine (Figure 11) similar to the methods previously reported in the literature [20, 69, 79, 82]. It should be noted that the resulting network could not be dissolved by applying heat and solvent. The solubility test (see *Supplementary Information*) showed that the network is insoluble after 24 hours at temperatures between 80-100 °C in THF, toluene and acetonitrile (Figure S8). The gel fractions from the solubility test remained above 98% for Vitrimer-S and Vitrimer-W and above 94% for Composite before and after first recycling step, which confirms the high and permanent cross-link density of the

materials. However, upon addition of butylamine, the network dissolves as a result of the exchange reaction. Thus, we used the following procedure: 0.39 g of Vitrimer-S were added to a vial containing 2 ml butylamine and 17 ml acetonitrile solvent and the solution was then stirred at 65 °C. As expected, addition of butylamine in the solvent resulted in a complete dissolution of the material due to amine exchange reaction. Finally, the obtained uncross-linked polymer chains were recovered by precipitation in 3× excess methanol. The GPC chromatogram of the original poly(AAEMA-*stat*-IBOMA) versus the recovered polymer shows the un-cross-linking process with a mono-functional amine and the recovery of polymer (Figure 11c). The recovered polymer had slightly higher molecular weight compared to the original polymer probably due to the branched structures and possible remaining cross-linked chains as previously observed in the literature [6]. However, possible side reactions should be taken into account as they result in irreversible cross-links or decomposition of the recycled material. ^{1}H NMR spectra of the recovered material (Figure S16) shows the characteristic peaks of the poly(AAEMA-*stat*-IBOMA) and butylamine and no significant changes on the recovered material after treatment with butylamine, which has been previously confirmed by Du Prez and coworkers [9] for the transamination of the vinylogous urethanes.

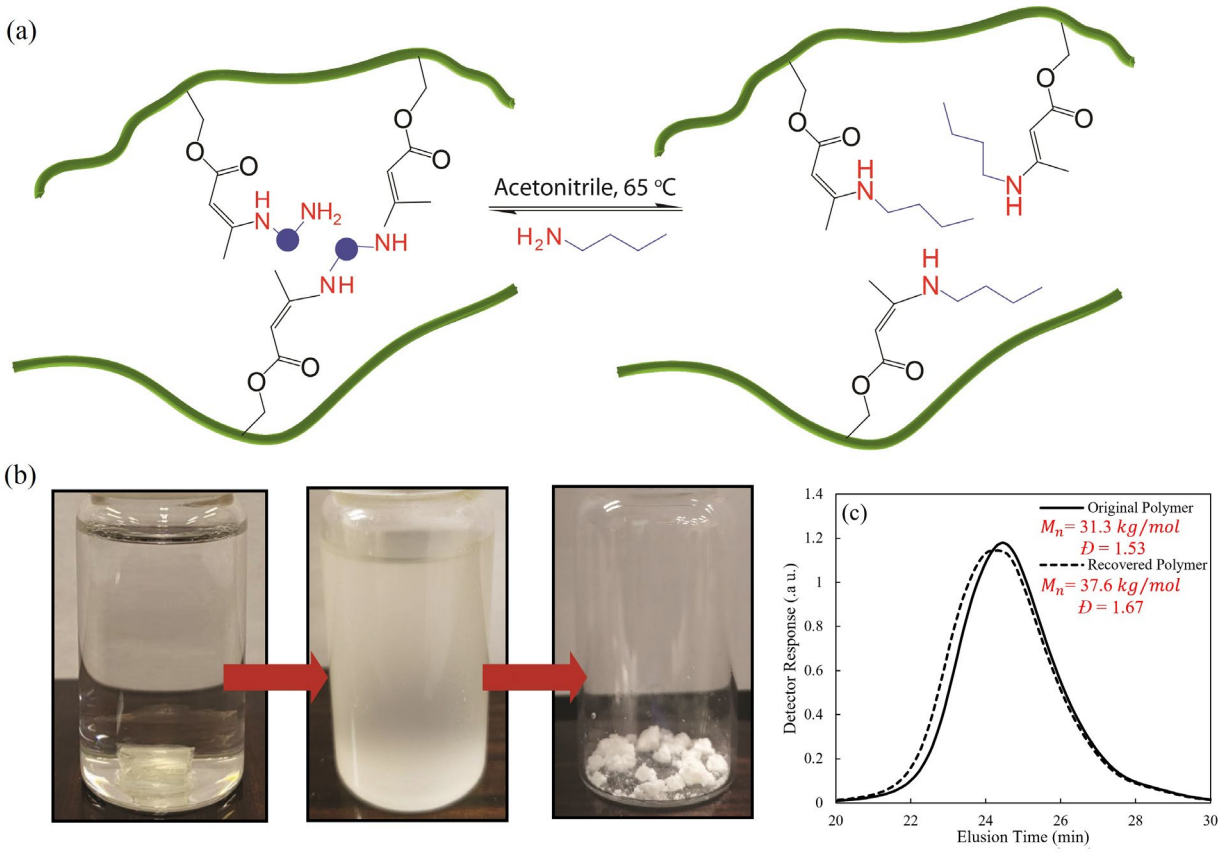

Figure 11. Un-cross-linking the network with mono-functional amine: (a) Schematic representation of dissolving the cross-linked polymer in presence of excess butylamine, (b) dissolved sample after treatment with butylamine at 65 °C and precipitation of the un-cross-linked polymer in methanol at room temperature, and (c) GPC chromatogram of the original vs recovered poly(AAEMA-*stat*-IBOMA).

Conclusions

We have demonstrated catalyst-free vinylogous urethane bio-based vitrimers and nanocomposite from AAEMA and IBOMA (a commercially available bio-based monomer) with potential applications in coatings and insulating materials. First, we explored NMP of poly(AAEMA-*stat*-IBOMA) and studied the polymerization kinetics. The reactivity ratios of the AAEMA/IBOMA pair in toluene at 100°C were found to be r_{AAEMA} = 1.43±0.05 and r_{IBOMA} = 0.79±0.03. To offer another useful route to obtain the same copolymers, we used nitroxide-mediated miniemulsion polymerization to synthesize the water-borne copolymers. Solution cast cross-linking using a bio-based bi-functional amine was used to synthesize the

cross-linked polymers. Improvement of thermal stability and tensile properties was achieved by adding amine-functionalized POSS nanoparticles to synthesize composite networks. Composite networks exhibited slower relaxation rates with higher apparent activation energy of stress relaxation compared to the neat vitrimer. Mechanical analysis and FTIR results confirmed the recyclability of vitrimers by hot press at 125 °C without appreciable changes in storage modulus and T_g after reprocessing. In order to further improve the mechanical properties, we suggest targeting higher M_n and T_g for the as-synthesized polymer as well as using multifunctional amines or multifunctional POSS in the vitrimer in the future. This dynamic process can be activated solely using elevated temperatures without using any catalysts. Finally, chemical un-cross-linking of the vitrimer was carried out by using butylamine, confirming that amine functional groups can be exchanged in a subsequent heat-activated transamination step. From a synthetic perspective, the ability to recycle a previously cross-linked polymer could reduce material waste and improve the economy of experimental designs.

Declaration of competing interest

The authors declare that they have no known competing financial interests or personal relationships that could have appeared to influence the work reported in this paper.

CRediT authorship contribution statement

F. Hajiali: Conceptualization, Investigation, Validation, Writing – original draft. **S. Tajbakhsh:** Investigation, Formal Analysis, Writing – Review & editing. **M. Marić:** Conceptualization, Supervision, Writing – Review & editing.

Acknowledgements

This research was supported by grants from the Natural Sciences and Engineering Research Council of Canada (Collaborative Research and Development (CRD) with Safran, Grant # CRDPJ-518396-17), PRIMA Quebec with Safran Cabin (Project # R15-46-004) and McGill Engineering Doctoral Award

(MEDA) scholarship from the Faculty of Engineering, McGill University. We also thank the Centre Québécois sur les Matériaux Fonctionnels (CQMF) for the use of the FTIR, DSC and TGA.

References

[1] J.-P. Pascault, H. Sautereau, J. Verdu, R.J. Williams, Thermosetting polymers, CRC press2002.
[2] N.T. Dintcheva, N. Jilov, F. La Mantia, Recycling of plastics from packaging, Polym. Degrad. Stabil. 57(2) (1997) 191-203.
[3] M. Capelot, D. Montarnal, F. Tournilhac, L. Leibler, Metal-catalyzed transesterification for healing and assembling of thermosets, J. Am. Chem. Soc. 134(18) (2012) 7664-7667.
[4] D. Montarnal, M. Capelot, F. Tournilhac, L. Leibler, Silica-like malleable materials from permanent organic networks, Science 334(6058) (2011) 965-968.
[5] W. Denissen, J.M. Winne, F.E. Du Prez, Vitrimers: permanent organic networks with glass-like fluidity, Chem. Sci. 7(1) (2016) 30-38.
[6] J.J. Lessard, L.F. Garcia, C.P. Easterling, M.B. Sims, K.C. Bentz, S. Arencibia, D.A. Savin, B.S. Sumerlin, Catalyst-Free Vitrimers from Vinyl Polymers, Macromolecules 52(5) (2019) 2105-2111.
[7] M. Röttger, T. Domenech, R. van der Weegen, A. Breuillac, R. Nicolaÿ, L. Leibler, High-performance vitrimers from commodity thermoplastics through dioxaborolane metathesis, Science 356(6333) (2017) 62-65.
[8] M. Capelot, M.M. Unterlass, F. Tournilhac, L. Leibler, Catalytic control of the vitrimer glass transition, ACS Macro Lett. 1(7) (2012) 789-792.
[9] W. Denissen, G. Rivero, R. Nicolaÿ, L. Leibler, J.M. Winne, F.E. Du Prez, Vinylogous urethane vitrimers, Adv. Funct. Mater. 25(16) (2015) 2451-2457.
[10] A.l. Legrand, C. Soulié-Ziakovic, Silica–epoxy vitrimer nanocomposites, Macromolecules 49(16) (2016) 5893-5902.
[11] L. Li, X. Chen, K. Jin, J.M. Torkelson, Vitrimers designed both to strongly suppress creep and to recover original cross-link density after reprocessing: quantitative theory and experiments, Macromolecules 51(15) (2018) 5537-5546.
[12] Z. Ma, Y. Wang, J. Zhu, J. Yu, Z. Hu, Bio-based epoxy vitrimers: Reprocessibility, controllable shape memory, and degradability, J. Polym. Sci. Polym. Chem. 55(10) (2017) 1790-1799.
[13] B. Hendriks, J. Waelkens, J.M. Winne, F.E. Du Prez, Poly (thioether) vitrimers via transalkylation of trialkylsulfonium salts, ACS Macro Lett. 6(9) (2017) 930-934.
[14] Y. Yang, Z. Pei, Z. Li, Y. Wei, Y. Ji, Making and remaking dynamic 3D structures by shining light on flat liquid crystalline vitrimer films without a mold, J. Am. Chem. Soc. 138(7) (2016) 2118-2121.
[15] N. Zheng, Z. Fang, W. Zou, Q. Zhao, T. Xie, Thermoset shape-memory polyurethane with intrinsic plasticity enabled by transcarbamoylation, Angew. Chem. Int. Ed. 55(38) (2016) 11421-11425.
[16] J.P. Brutman, P.A. Delgado, M.A. Hillmyer, Polylactide vitrimers, ACS Macro lett. 3(7) (2014) 607-610.
[17] Y. Yang, Z. Pei, X. Zhang, L. Tao, Y. Wei, Y. Ji, Carbon nanotube–vitrimer composite for facile and efficient photo-welding of epoxy, Chem. Sci. 5(9) (2014) 3486-3492.
[18] D.J. Fortman, J.P. Brutman, C.J. Cramer, M.A. Hillmyer, W.R. Dichtel, Mechanically activated, catalyst-free polyhydroxyurethane vitrimers, J. Am. Chem. Soc. 137(44) (2015) 14019-14022.
[19] Z. Pei, Y. Yang, Q. Chen, E.M. Terentjev, Y. Wei, Y. Ji, Mouldable liquid-crystalline elastomer actuators with exchangeable covalent bonds, Nat. Mater. 13(1) (2014) 36.
[20] W. Denissen, I. De Baere, W. Van Paepegem, L. Leibler, J. Winne, F.E. Du Prez, Vinylogous Urea Vitrimers and Their Application in Fiber Reinforced Composites, Macromolecules 51(5) (2018) 2054-2064.

[21] T. Stukenbroeker, W. Wang, J.M. Winne, F.E. Du Prez, R. Nicolaÿ, L. Leibler, Polydimethylsiloxane quenchable vitrimers, Polym. Chem. 8(43) (2017) 6590-6593.
[22] Y. Nishimura, J. Chung, H. Muradyan, Z. Guan, Silyl ether as a robust and thermally stable dynamic covalent motif for malleable polymer design, J. Am. Chem. Soc. 139(42) (2017) 14881-14884.
[23] W.A. Ogden, Z. Guan, Recyclable, strong, and highly malleable thermosets based on boroxine networks, J. Am. Chem. Soc. 140(20) (2018) 6217-6220.
[24] P. Taynton, K. Yu, R.K. Shoemaker, Y. Jin, H.J. Qi, W. Zhang, Heat-or Water-Driven Malleability in a Highly Recyclable Covalent Network Polymer, Adv. Mater. 26(23) (2014) 3938-3942.
[25] A. Rekondo, R. Martin, A.R. de Luzuriaga, G. Cabañero, H.J. Grande, I. Odriozola, Catalyst-free room-temperature self-healing elastomers based on aromatic disulfide metathesis, Mater. Horiz. 1(2) (2014) 237-240.
[26] Y.-X. Lu, Z. Guan, Olefin metathesis for effective polymer healing via dynamic exchange of strong carbon–carbon double bonds, J. Am. Chem. Soc. 134(34) (2012) 14226-14231.
[27] Y.-X. Lu, F. Tournilhac, L. Leibler, Z. Guan, Making insoluble polymer networks malleable via olefin metathesis, J. Am. Chem. Soc. 134(20) (2012) 8424-8427.
[28] W. Denissen, M. Droesbeke, R. Nicolaÿ, L. Leibler, J.M. Winne, F.E. Du Prez, Chemical control of the viscoelastic properties of vinylogous urethane vitrimers, Nat. Commun. 8 (2017) 14857.
[29] J.J. Lessard, G.M. Scheutz, S.H. Sung, K.A. Lantz, T.H. Epps, B.S. Sumerlin, Block Copolymer Vitrimers, J. Am. Chem. Soc. 142(1) (2020) 283-289.
[30] P. Taynton, H. Ni, C. Zhu, K. Yu, S. Loob, Y. Jin, H.J. Qi, W. Zhang, Repairable woven carbon fiber composites with full recyclability enabled by malleable polyimine networks, Adv. Mater. 28(15) (2016) 2904-2909.
[31] E. Chabert, J. Vial, J.-P. Cauchois, M. Mihaluta, F. Tournilhac, Multiple welding of long fiber epoxy vitrimer composites, Soft Matter 12(21) (2016) 4838-4845.
[32] A.R. de Luzuriaga, R. Martin, N. Markaide, A. Rekondo, G. Cabañero, J. Rodríguez, I. Odriozola, Epoxy resin with exchangeable disulfide crosslinks to obtain reprocessable, repairable and recyclable fiber-reinforced thermoset composites, Mater. Horiz. 3(3) (2016) 241-247.
[33] L. Bai, J. Zheng, Robust, reprocessable and shape-memory vinylogous urethane vitrimer composites enhanced by sacrificial and self-catalysis Zn(II)–ligand bonds, Compos. Sci. Technol. 190 (2020) 108062.
[34] C.-T. Lin, S.-W. Kuo, C.-F. Huang, F.-C. Chang, Glass transition temperature enhancement of PMMA through copolymerization with PMAAM and PTCM mediated by hydrogen bonding, Polymer 51(4) (2010) 883-889.
[35] S.-W. Kuo, H.-T. Tsai, Complementary Multiple Hydrogen-Bonding Interactions Increase the Glass Transition Temperatures to PMMA Copolymer Mixtures, Macromolecules 42(13) (2009) 4701-4711.
[36] J. Liu, R.C. Li, G.J. Sand, V. Bulmus, T.P. Davis, H.D. Maynard, Keto-functionalized polymer scaffolds as versatile precursors to polymer side-chain conjugates, Macromolecules 46(1) (2013) 8-14.
[37] J. Nicolas, Y. Guillaneuf, C. Lefay, D. Bertin, D. Gigmes, B. Charleux, Nitroxide-mediated polymerization, Prog. Polym. Sci. 38(1) (2013) 63-235.
[38] F. Hajiali, A. Métafiot, L. Benitez-Ek, L. Alloune, M. Marić, Nitroxide mediated polymerization of sustainably sourced isobornyl methacrylate and tridecyl methacrylate with acrylonitrile co-monomer, J. Polym. Sci. Polym. Chem. 56(21) (2018) 2422-2436.
[39] N. Ballard, M. Aguirre, A. Simula, A. Agirre, J.R. Leiza, J.M. Asua, S. van Es, New Class of Alkoxyamines for Efficient Controlled Homopolymerization of Methacrylates, ACS Macro Lett. 5(9) (2016) 1019-1022.
[40] N. Ballard, A. Simula, M. Aguirre, J.R. Leiza, S. van Es, J.M. Asua, Synthesis of poly(methyl methacrylate) and block copolymers by semi-batch nitroxide mediated polymerization, Polym. Chem. 7(45) (2016) 6964-6972.
[41] R. Batlaw, P.D. Moore, Printing ink emulsion having reduced VOC, Google Patents, 1995.
[42] S. Tajbakhsh, F. Hajiali, M. Marić, Nitroxide-Mediated Miniemulsion Polymerization of Bio-Based Methacrylates, Ind. Eng. Chem. Res. 59(19) (2020) 8921-8936.

[43] F. Chauvin, P.-E. Dufils, D. Gigmes, Y. Guillaneuf, S.R.A. Marque, P. Tordo, D. Bertin, Nitroxide-Mediated Polymerization: The Pivotal Role of the kd Value of the Initiating Alkoxyamine and the Importance of the Experimental Conditions, Macromolecules 39(16) (2006) 5238-5250.
[44] G. Moad, D.H. Solomon, The chemistry of radical polymerization, Elsevier2006.
[45] A. Simula, N. Ballard, M. Aguirre, J.R. Leiza, S. van Es, J.M. Asua, Nitroxide mediated copolymerization of acrylates, methacrylates and styrene: The importance of side reactions in the polymerization of acrylates, European Polymer Journal 110 (2019) 319-329.
[46] N. Ballard, M. Aguirre, A. Simula, J.R. Leiza, S. van Es, J.M. Asua, High solids content nitroxide mediated miniemulsion polymerization of n-butyl methacrylate, Polymer Chemistry 8(10) (2017) 1628-1635.
[47] A. Simula, M. Aguirre, N. Ballard, A. Veloso, J.R. Leiza, S. van Es, J.M. Asua, Novel alkoxyamines for the successful controlled polymerization of styrene and methacrylates, Polymer Chemistry 8(10) (2017) 1728-1736.
[48] S. Beuermann, M. Buback, T.P. Davis, N. García, R.G. Gilbert, R.A. Hutchinson, A. Kajiwara, M. Kamachi, I. Lacík, G.T. Russell, Critically Evaluated Rate Coefficients for Free-Radical Polymerization, 4, Macromol. Chemi. Phys. 204(10) (2003) 1338-1350.
[49] A. Zoller, K.B. Kockler, M. Rollet, C. Lefay, D. Gigmes, C. Barner-Kowollik, Y. Guillaneuf, A complete kinetic study of a versatile functional monomer: acetoacetoxyethyl methacrylate (AAEMA), Polym. Chem. 7(35) (2016) 5518-5525.
[50] V.E. Meyer, G.G. Lowry, Integral and differential binary copolymerization equations, J. Polym. Sci. A 3(8) (1965) 2843-2851.
[51] I. Skeist, Copolymerization: the composition distribution curve, J. Am. Chem. Soc. 68(9) (1946) 1781-1784.
[52] S. Pal, B. Banoth, G. Rahithya, A. Dhawan, P. De, Copolyperoxides of 2-(acetoacetoxy) ethyl methacrylate with methyl methacrylate and styrene; Synthesis, characterization, thermal analysis, and reactivity ratios, Polymer 53(13) (2012) 2583-2590.
[53] F. Hajiali, A. Shojaei, Network structure and mechanical properties of polydimethylsiloxane filled with nanodiamond–Effect of degree of silanization of nanodiamond, Compos. Sci. Technol. 142 (2017) 227-234.
[54] S. Tajbakhsh, F. Hajiali, A comprehensive study on the fabrication and properties of biocomposites of poly (lactic acid)/ceramics for bone tissue engineering, Mater. Sci. Eng. C 70 (2017) 897-912.
[55] X. Chen, L. Li, T. Wei, D.C. Venerus, J.M. Torkelson, Reprocessable polyhydroxyurethane network composites: effect of filler surface functionality on cross-link density recovery and stress relaxation, ACS applied materials & interfaces 11(2) (2018) 2398-2407.
[56] S. Schäfer, G. Kickelbick, Double Reversible Networks: Improvement of Self-Healing in Hybrid Materials via Combination of Diels–Alder Cross-Linking and Hydrogen Bonds, Macromolecules 51(15) (2018) 6099-6110.
[57] M. Qiu, S. Wu, Z. Tang, B. Guo, Exchangeable interfacial crosslinks towards mechanically robust elastomer/carbon nanotubes vitrimers, Compos. Sci. Technol. 165 (2018) 24-30.
[58] Z. Huang, Y. Wang, J. Zhu, J. Yu, Z. Hu, Surface engineering of nanosilica for vitrimer composites, Compos. Sci. Technol. 154 (2018) 18-27.
[59] N.J. Van Zee, R. Nicolaÿ, Vitrimers: Permanently crosslinked polymers with dynamic network topology, Prog. Polym. Sci. 104 (2020) 101233.
[60] S. Tajbakhsh, M. Marić, Nitroxide mediated miniemulsion polymerization of methacryloisobutyl POSS: Homopolymers and copolymers with alkyl methacrylates, J. Polym. Sci. 2020; 58: 2741– 2754.
[61] E. Kharlampieva, V. Kozlovskaya, B. Wallet, V.V. Shevchenko, R.R. Naik, R. Vaia, D.L. Kaplan, V.V. Tsukruk, Co-cross-linking Silk Matrices with Silica Nanostructures for Robust Ultrathin Nanocomposites, ACS Nano 4(12) (2010) 7053-7063.
[62] R. Gunawidjaja, F. Huang, M. Gumenna, N. Klimenko, G.A. Nunnery, V. Shevchenko, R. Tannenbaum, V.V. Tsukruk, Bulk and Surface Assembly of Branched Amphiphilic Polyhedral Oligomer Silsesquioxane Compounds, Langmuir 25(2) (2009) 1196-1209.

[63] D. Gnanasekaran, A. Shanavas, W.W. Focke, R. Sadiku, Polyhedral oligomeric silsesquioxane/polyamide bio-nanocomposite membranes: structure-gas transport properties, RSC Adv. 5(15) (2015) 11272-11283.
[64] J. Huang, C. He, X. Liu, J. Xu, C.S.S. Tay, S.Y. Chow, Organic–inorganic nanocomposites from cubic silsesquioxane epoxides: direct characterization of interphase, and thermomechanical properties, Polymer 46(18) (2005) 7018-7027.
[65] M. Oaten, N.R. Choudhury, Silsesquioxane− Urethane hybrid for thin film applications, Macromolecules 38(15) (2005) 6392-6401.
[66] R.A. Mantz, P.F. Jones, K.P. Chaffee, J.D. Lichtenhan, J.W. Gilman, I.M.K. Ismail, M.J. Burmeister, Thermolysis of Polyhedral Oligomeric Silsesquioxane (POSS) Macromers and POSS−Siloxane Copolymers, Chem. Mater. 8(6) (1996) 1250-1259.
[67] T. Calvo-Correas, M.D. Martin, A. Retegi, N. Gabilondo, M.A. Corcuera, A. Eceiza, Synthesis and Characterization of Polyurethanes with High Renewable Carbon Content and Tailored Properties, ACS Sustain. Chem. Eng. 4(10) (2016) 5684-5692.
[68] Y. Liu, Z. Tang, Y. Chen, C. Zhang, B. Guo, Engineering of β-Hydroxyl Esters into Elastomer–Nanoparticle Interface toward Malleable, Robust, and Reprocessable Vitrimer Composites, ACS Appl. Mater. Interfaces 10(3) (2018) 2992-3001.
[69] S. Dhers, G. Vantomme, L. Avérous, A fully bio-based polyimine vitrimer derived from fructose, Green Chemistry 21(7) (2019) 1596-1601.
[70] M. Guerre, C. Taplan, J.M. Winne, F.E. Du Prez, Vitrimers: directing chemical reactivity to control material properties, Chem. Sci. 11(19) (2020) 4855-4870.
[71] M. Guerre, C. Taplan, J.M. Winne, F.E. Du Prez, Vitrimers: directing chemical reactivity to control material properties, Chem. Sci. 11 (2020) 4855-4870.
[72] M.M. Obadia, B.P. Mudraboyina, A. Serghei, D. Montarnal, E. Drockenmuller, Reprocessing and recycling of highly cross-linked ion-conducting networks through transalkylation exchanges of C–N bonds, J. Am. Chem. Soc. 137(18) (2015) 6078-6083.
[73] J.A. Brydson, Plastics materials, Elsevier1999.
[74] L. Petton, A.E. Ciolino, B. Dervaux, F.E. Du Prez, From one-pot stabilisation to in situ functionalisation in nitroxide mediated polymerisation: an efficient extension towards atom transfer radical polymerisation, Polym. Chem. 3(7) (2012) 1867-1878.
[75] F. Hajiali, M. Marić, Incorporation of POSS to improve thermal stability of bio-based polymethacrylates by nitroxide-mediated polymerization: Polymerization kinetics and characterization, J. Polym. Sci. 58(11) (2020) 1503-1520.
[76] J. Nicolas, S. Brusseau, B. Charleux, A minimal amount of acrylonitrile turns the nitroxide-mediated polymerization of methyl methacrylate into an almost ideal controlled/living system, J. Polym. Sci. A Polym. Chem. 48(1) (2010) 34-47.
[77] F. Hajiali, S. Tajbakhsh, M. Marić, Thermal Characteristics and Flame Retardance Behavior of Phosphoric Acid-Containing Poly(Methacrylates) Synthesized by RAFT Polymerization, Mater. Today Commun. (2020) 101618.
[78] Y. Spiesschaert, M. Guerre, L. Imbernon, J.M. Winne, F. Du Prez, Filler reinforced polydimethylsiloxane-based vitrimers, Polymer 172 (2019) 239-246.
[79] Z. Liu, C. Zhang, Z. Shi, J. Yin, M. Tian, Tailoring vinylogous urethane chemistry for the cross-linked polybutadiene: Wide freedom design, multiple recycling methods, good shape memory behavior, Polymer 148 (2018) 202-210.
[80] I. Yilgor, T. Eynur, E. Yilgor, G.L. Wilkes, Contribution of soft segment entanglement on the tensile properties of silicone–urea copolymers with low hard segment contents, Polymer 50(19) (2009) 4432-4437.
[81] M. Guerre, C. Taplan, R. Nicolaÿ, J.M. Winne, F.E. Du Prez, Fluorinated Vitrimer Elastomers with a Dual Temperature Response, J. Am. Chem. Soc. 140(41) (2018) 13272-13284.
[82] X. Kuang, Y. Zhou, Q. Shi, T. Wang, H.J. Qi, Recycling of epoxy thermoset and composites via good solvent assisted and small molecules participated exchange reactions, ACS Sustain. Chem. Eng. 6(7) (2018) 9189-9197.